Applied Catalysis B: Environmental 156–157 (2014) 94–100

Contents lists available at ScienceDirect

Applied Catalysis B: Environmental

journal homepage: www.elsevier.com/locate/apcatb

TCE abatement with a plasma-catalytic combined system using MnO_2 as catalyst

A.M. Vandenbroucke[a,*], M. Mora[b], C. Jiménez-Sanchidrián[b], F.J. Romero-Salguero[b], N. De Geyter[a], C. Leys[a], R. Morent[a]

[a] Research Unit Plasma Technology (RUPT), Department of Applied Physics, Faculty of Engineering and Architecture, Ghent University, Sint-Pietersnieuwstraat 41, B-9000 Ghent, Belgium

[b] Department of Organic Chemistry, Faculty of Sciences, University of Córdoba, Campus de Rabanales, Marie Curie Building, Ctra. Nnal. IV, km 396, 14071 Córdoba, Spain

ARTICLE INFO

Article history:
Received 24 September 2013
Received in revised form 26 February 2014
Accepted 4 March 2014
Available online 13 March 2014

Keywords:
Non-thermal plasma
Catalysis
Plasma-catalysis
Volatile organic compound
Manganese oxide

ABSTRACT

A multi-pin-to-plate negative DC corona/glow discharge combined with MnO_2 catalyst placed downstream of the plasma reactor was experimentally investigated for the abatement of trichloroethylene (TCE) in dry air. For the plasma alone system even at 240 J/L, the CO_x-selectivity did not exceed 15%, due to the formation of oxygenated intermediates (phosgene, dichloroacetylchloride). However, by combining both systems, the TCE abatement was improved and the selectivity of the process was greatly enhanced towards total oxidation. For the plasma-catalytic system, the activation energy (1.5 kcal/mol) was significantly decreased compared to pure catalytic conditions (8.7 kcal/mol), suggesting that the oxygenated intermediates produced by the plasma are more susceptible for catalytic oxidation than TCE. Furthermore, the ozone produced by the plasma is able to dissociate on the catalyst surface by a Rideal–Eley mechanism, thereby creating peroxide surface groups which greatly improve the oxidation of TCE. Based on the experimental results, a reaction pathway for the plasma-catalytic TCE abatement is suggested.
© 2014 Elsevier B.V. All rights reserved.

1. Introduction

Air pollution has become a global issue that endangers the condition of the environment and poses serious health risks. In this regard, volatile organic compounds (VOCs) are a large group of chemical compounds that have a significant contribution to poor air quality in many populated areas. Several kinds of VOCs are very harmful to human health because of their carcinogenic and mutagenic effects, while many environmental problems are related to their presence in the soil, groundwater and atmosphere. Therefore, air quality regulations are tightened and new remediation technologies are being explored in order to overcome these problems.

As an alternative to conventional air purification methods, such as adsorption and thermal/catalytic oxidation, non-thermal plasma (NTP) technology has been investigated for the removal of dilute VOCs from waste gases and indoor air since the last 2 decades [1–7]. In a NTP, electrons are selectively accelerated by applying a sufficiently strong electric field. These highly energetic electrons (1–10 eV) trigger multiple chemical processes such as ionization, excitation and dissociation through collisions with neutral background molecules (N_2, O_2, H_2O). Hence, air pollutants are being exposed to a reactive chemical environment containing ions, radicals, excited species and metastable states by which they are converted to less harmful products. The use of NTP for air purification has several desirable features resulting from its operating conditions; such as a quick start-up, rapid response to changes in the composition of the waste gas and operation at ambient conditions which excludes the use of expensive vacuum systems. Furthermore, NTP systems can effectively be combined with other established technologies.

Especially the combination of NTP with heterogeneous catalysis has gained increased interest. The introduction of a catalyst, either inside or downstream of a NTP reactor, leads to an enhancement of the energy efficiency, carbon balance and mineralization degree compared to plasma alone systems. Recently, Vandenbroucke et al. have extensively reviewed the recent achievements and current status of this hybrid technology for VOC abatement [8].

For the removal of VOCs with NTP, the formation and emission of large amounts of ozone is a serious drawback because O_3 is responsible for respiratory diseases and is implied in the formation of photochemical smog. To prevent the emission of ozone, several catalytic formulations have been tested. It is found that p-type

* Corresponding author. Tel.: +32 9 264 38 38.
E-mail address: ArneM.Vandenbroucke@UGent.be (A.M. Vandenbroucke).

http://dx.doi.org/10.1016/j.apcatb.2014.03.007
0926-3373/© 2014 Elsevier B.V. All rights reserved.

oxide semiconductors are the most active substances for ozone decomposition [9,10]. Among these, MnO_2 has shown to possess the most interesting properties, such as ease of synthesizing crystalline phases [11] and the mobility of oxygen in the crystal lattice, creating vacancies which promote the formation of oxygen groups at the catalyst surface [12]. This make them appropriate materials for VOC oxidation reactions [13].

Several groups have investigated the performance of MnO_2 combined with NTP for VOC removal. Futamura and Gurusamy observed synergistic effects for the decomposition of fluorinated hydrocarbons with dielectric barrier discharge (DBD) reactors filled with MnO_2 [14]. Jarrige and Vervisch coupled a pulsed corona discharge with a fixed catalytic bed of MnO_2/Al_2O_3 downstream [15]. At ambient temperature, ozone was almost completely decomposed by the catalyst, producing reactive oxygen species leading to a greatly enhanced conversion and CO_2-selectivity for the removal of propane. Han et al. also investigated the use of MnO_2 downstream of a DBD reactor and reported a significant improvement of the energy efficiency at low energy input [16].

The aim of this paper is to study the opportunities of a plasma-catalytic system with MnO_2 downstream for the abatement of TCE, in terms of conversion and CO_x-selectivity. Also, special attention is given to the effect of catalyst temperature and the role of ozone in the plasma-catalytic TCE abatement. Finally, a degradation scheme is proposed for the destruction of TCE in the gas-phase and on the catalyst surface, which is innovative in comparison to the latter studies.

2. Experimental

Fig. 1 shows a schematic diagram of the experimental set-up. A bottle of dry synthetic air (Alphagaz 1, Air Liquide) was connected to two mass flow controllers (MFC). Next, air was fed to a TCE bubbling bottle located in an ice-water bath. The initial TCE concentration was controlled by the feed gas flow rate. All experiments were carried out with a total air flow of 500 mL/min containing 500 ppm TCE. The TCE abatement and the identification of by-products were determined with a FT-IR spectrometer (Bruker, Vertex 70). The optical length of the gas cell and the resolution of the spectrometer were set at 20 cm and 4 cm^{-1}, respectively. Spectra were taken after steady state condition and consisted of 10 averaged measurements. The mercury–cadmium–telluride (MCT) detector of the FT-IR was cooled with liquid nitrogen. OPUS (Bruker) software was used to collect and analyze the obtained spectra. The formation of ozone was analyzed by an UV ozone monitor (Envitec, model 450).

The plasma source is based on the concept of a multi-pin-to-plate negative DC corona/glow discharge [17,18]. The rectangular duct of the reactor has a cross section of 40 mm × 9 mm and a length of 400 mm. The plasma source consists of 10 aligned cathode pins which were positioned 28 mm from each other. The distance between the 10 cathode pins and the single anode plate is 10 mm. The discharge is powered with a DC power supply (Technix, SR40-R-1200) and generated at atmospheric pressure and room temperature. During experiments, the energy density of the plasma (i.e. the ratio of the plasma input power to gas flow rate) is changed by varying the plasma voltage. A high voltage probe (Fluke 80 K-40, division ratio 1/1000) measures the voltage applied to the inner electrode. The discharge current is determined by recording the voltage signal across a 100 Ω resistor placed in series between the counter electrode and ground. The plasma voltage and discharge current varied between 8.0–10.5 kV and 0.04–0.20 mA, respectively. The spherical surface segments in the anode plate have a radius of curvature of 17.5 mm and a depth of 5.0 mm. Stable and uniform discharge operation is ensured by the gas flow and by ballasting each cathode pin with a 1.5 MΩ resistor. The fraction of the total electrical power that is dissipated in these resistors amounts to 10% at most.

Manganese oxide was purchased from Panreac. Before its use, it was calcinated for 4 h at 500 °C under a stream of dry synthetic air with a flow of 200 mL/min. For all tests, 1 g of MnO_2 powder was introduced in a cylindrical glass reactor located in a temperature controlled vertical tubular oven operating in the temperature range of 300–500 °C. The reactor was made in Pyrex glass and had an inner diameter of 20 mm and an effective length of 100 mm. With these conditions, the space velocity reached 30,000 h^{-1}. The oven was heated in a period of 60 min to the desired value. The measurements were then performed after thermal balance was reached.

3. Results and discussion

To investigate the performance of the combined plasma-catalytic system, both parts are initially considered separately, i.e. destruction of TCE through the use of NTP and via catalytic oxidation. To evaluate the process, the following parameters are employed:

The TCE abatement is calculated from:

$$\text{TCE abatement}(\%) = \left(\frac{[\text{TCE}]_{\text{in}} - [\text{TCE}]_{\text{out}}}{[\text{TCE}]_{\text{in}}}\right) \times 100 \qquad (1)$$

where $[\text{TCE}]_{\text{in}}$ is the concentration introduced in the reactor and $[\text{TCE}]_{\text{out}}$ is the concentration in the effluent gas.

The selectivities of CO, CO_2, CO_x and chlorinated by-products are defined as:

$$S_{\text{CO}}(\%) = \frac{[\text{CO}]}{(2 \times [\text{TCE}]_{\text{conv}})} \times 100 \qquad (2)$$

$$S_{\text{CO}_2}(\%) = \frac{[\text{CO}_2]}{(2 \times [\text{TCE}]_{\text{conv}})} \times 100 \qquad (3)$$

$$S_{\text{CO}_x}(\%) = S_{\text{CO}} + S_{\text{CO}_2} \qquad (4)$$

$$S_{\text{Cl by-products}}(\%) = 100 - S_{\text{CO}_x} \qquad (5)$$

where [CO] and $[CO_2]$ are the concentrations of carbon monoxide and carbon dioxide detected in the effluent gas as a result of TCE oxidation and $[\text{TCE}]_{\text{conv}}$ is the concentration of TCE converted by the process.

3.1. TCE abatement using non-thermal plasma

The abatement of TCE with the plasma system alone was investigated for a gas flow rate of 500 mL/min dry air containing 500 ppm TCE. Fig. 2 shows the TCE abatement and the selectivity to CO, CO_2 and chlorinated by-products in the plasma as a function of the energy density.

As expected, an increase of the energy density in the plasma led to an enhanced TCE abatement. For a maximum energy density of 240 J/L the TCE abatement reached 85%. This conversion was however related to the formation of undesirable chlorinated by-products such as phosgene ($COCl_2$) and dichloroacetylchloride (DCAC) [19]. Also, the increase of energy density in the plasma gave an increase of the selectivity to CO and CO_2. Nevertheless, these selectivities were only 15% at 240 J/L. According to Kirkpatrick et al. [20], DCAC is the major by-product of TCE decomposition with NTP due to reaction of TCE with ClO radicals (generated in situ by decomposition of the same VOC in the plasma) according to the following reaction:

$$C_2HCl_3 + ClO^\bullet \rightarrow CHCl_2COCl + Cl^\bullet$$

The low selectivity's to CO and CO_2 can be rationalized if we consider a study by Futamura and Yamamoto [21], which refers

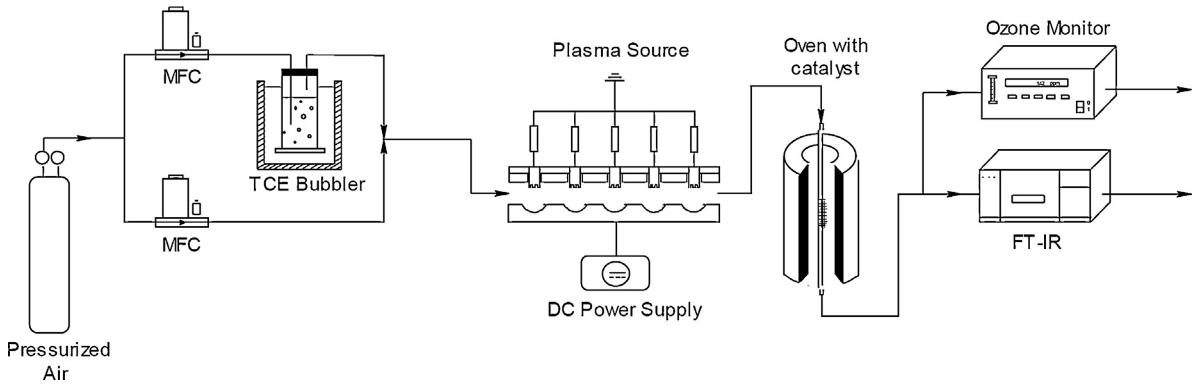

Fig. 1. Schematic diagram of the experimental set-up.

to the formation of peroxide radicals in the plasma, which would result in oxidative VOC decomposition to CO and CO_2:

$$R* + O_2 \rightarrow ROO* \rightarrow \text{reactionintermediates} \rightarrow CO, CO_2$$

3.2. TCE abatement using MnO_2 as catalyst

MnO_2 has been chosen as catalyst due to its excellent results for the oxidation of different VOCs, such as formaldehyde/methanol [22], cyclohexane [4] and benzene/toluene [5]. As the performance of a catalyst depends on the operating temperature, we chose a wide range of temperatures (300–500 °C) in order to monitor both the TCE abatement and its selectivity to the various reaction products.

As shown in Fig. 3, a higher temperature favored the TCE abatement, which exhibited a maximum of 42.6% at 500 °C. Also, a large increase was observed for the CO_x-selectivity when comparing both systems, NTP and catalytic reactor, separately, reaching 98% at higher catalyst temperatures, thereby minimizing the formation of chlorinated by-products. This result is quite expected considering that the catalyst can produce the following total oxidation reactions for TCE [23]:

$$C_2HCl_3 + 2O_2 \rightarrow 2CO_2 + HCl + Cl_2$$

$$C_2HCl_3 + O_2 \rightarrow 2CO + HCl + Cl_2$$

The catalytic activity of the oxide is related to several factors. One of the most important factors is related to the reaction temperature (catalytic furnace temperature) and the oxygen mobility in the crystal lattice of the solid, i.e. the presence of a large number of crystal defects [24].

3.3. TCE abatement using the plasma-catalytic combined system

The plasma-catalytic experiments were performed at different values of energy density of the plasma (40–240 J/L) and the catalyst temperature was fixed at 300 °C (Fig. 4). The combined system enhanced the TCE abatement compared to the plasma reactor, obtaining a value of 90.5% (plasma-catalysis) versus 84.5% (plasma) at 240 J/L. The abatement of TCE in the catalyst system alone operating at 300 °C was only 9.3%. The selectivity of the catalytic and combined system is shown at the bottom of Fig. 4. At low energy density, the combined system improves the CO_x-selectivity (62.5%) compared to the catalyst alone case (56%), although for higher energy densities there is no real enhancement noticeable. Therefore, experiments should be performed in order to further optimize the combined system and to improve the selectivity of the process. However, at this point, we can conclude that the combined system is an effective method for the abatement of TCE.

The formation of various reaction products was evaluated in the plasma-catalytic system at different oven temperatures. The next step was to study the plasma-catalytic abatement of TCE using the same temperature range (300–500 °C) but applying low energy density (40 and 80 J/L) to improve the energy efficiency of the entire system.

Fig. 5 shows TCE abatement and selectivity to different products for MnO_2 and the plasma-catalytic system. The TCE abatement increased with respect to the temperature in the furnace, obtaining the best value for an energy density of 80 J/L and maximum temperature of 500 °C (78%). The CO_x-selectivity depends on the oven temperature but is not much affected by the applied energy density. At 500 °C, the combined system slightly improves the CO_x-selectivity while at 300 °C there is no distinct effect. If we consider the selectivity to CO and CO_2, we also find different situations depending on the presence or the absence of the plasma in the

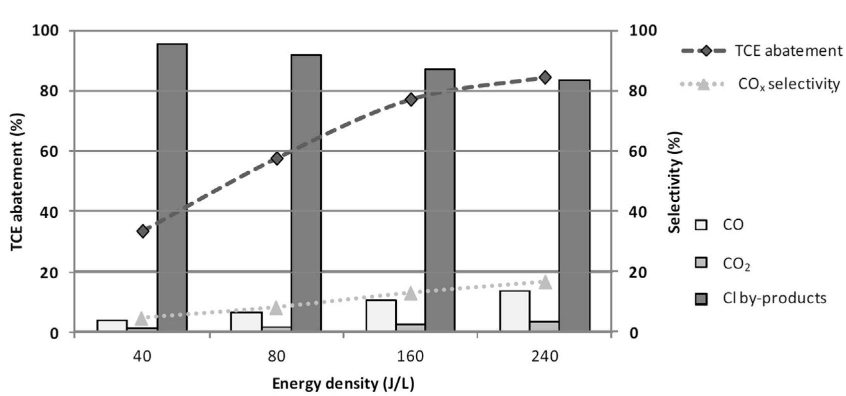

Fig. 2. TCE abatement with non-thermal plasma.

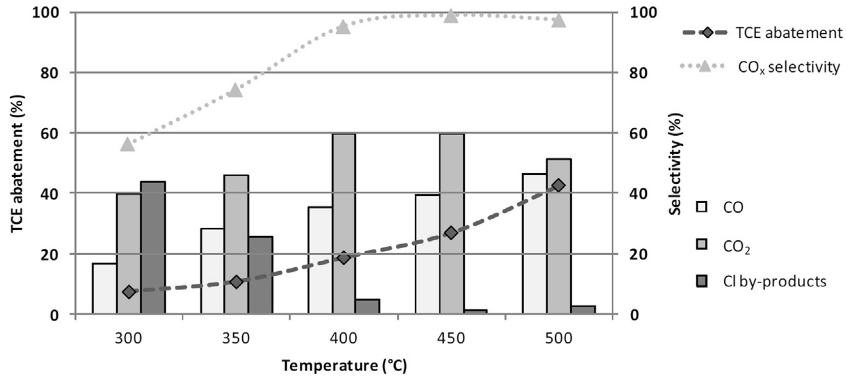

Fig. 3. TCE abatement with MnO_2.

destruction of TCE. Thus, if only the catalyst acts, we have that more CO_2 is produced than CO, while we have the opposite effect when also plasma is involved. Moreover, in the whole temperature range, the combination of plasma and catalysis is the optimal combination to get the best production values of CO and CO_2.

3.4. Calculation of the activation energy for TCE abatement with plasma-catalysis

According to the previous results on the combined system, the use of plasma has a beneficial effect on the performance of the catalyst. In order to examine if the plasma provides an extra activation of the catalyst, Arrhenius plots were used to calculate the activation energy (E_a) of the three systems (Fig. 6).

For the catalytic abatement, large temperature dependence was observed with respect to the total conversion. The calculated activation energy of 8.67 kcal/mol is in agreement with earlier results obtained for catalytic TCE oxidation [25]. However, in case of plasma-catalysis, the total conversion is much less dependent of the temperature. From these results, it clearly seems that the plasma participates in the transformation of TCE. This also suggests that there is a positive interaction of intermediate oxidation products (phosgene, DCAC) with the catalyst surface. Although this mechanism is not fully elucidated yet, it is reasonable to consider that these intermediates are capable of reaching the catalyst surface. Because these molecules are more susceptible to oxidation by MnO_2, the activation energy is significantly reduced when compared to catalytic oxidation.

3.5. Synergy factor in the TCE abatement by plasma-catalysis

Previous studies have shown that the combination of NTP with heterogeneous catalysis often induces a synergetic effect on the removal efficiency of the entire process [26–31]. To evaluate the synergy in our process, we introduce a synergy factor f for TCE abatement, as well as for CO and CO_2 yield, which are calculated as followed:

$$f_{TCE} = \frac{(\text{TCE abatement})_{\text{plasma-catalysis}}}{[(\text{TCE abatement})_{\text{plasma}} + (\text{TCE abatement})_{\text{catalysis}}]} \quad (8)$$

$$f_{CO} = \frac{(Y_{CO})_{\text{plasma-catalysis}}}{[(Y_{CO})_{\text{plasma}} + (Y_{CO})_{\text{catalysis}}]} \quad (9)$$

$$f_{CO_2} = \frac{(Y_{CO_2})_{\text{plasma-catalysis}}}{[(Y_{CO_2})_{\text{plasma}} + (Y_{CO_2})_{\text{catalysis}}]} \quad (10)$$

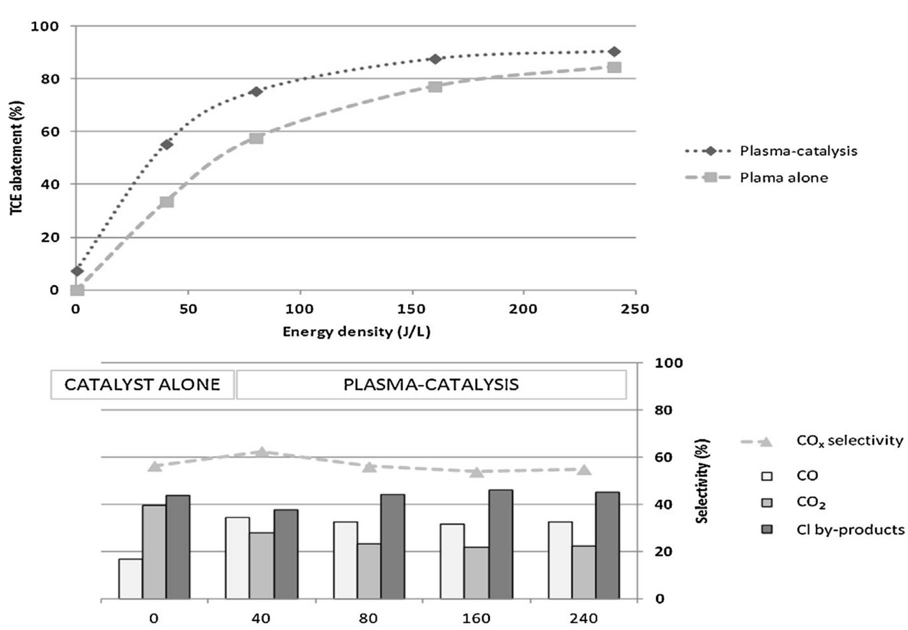

Fig. 4. TCE abatement with the plasma-catalytic (MnO_2) combined system (oven temperature 300 °C).

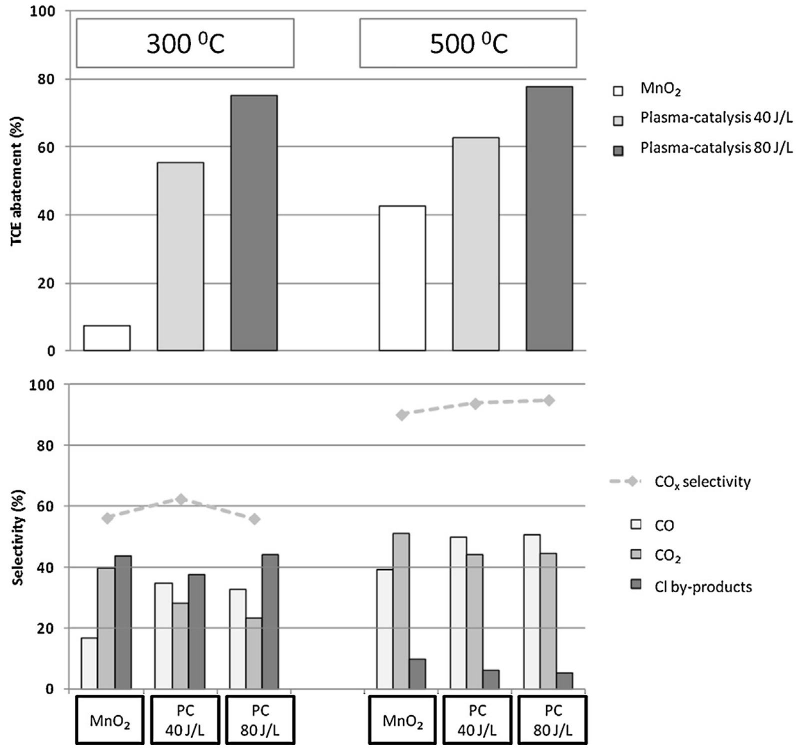

Fig. 5. Influence of the energy density on TCE abatement and selectivity with the plasma-catalytic combined system.

and where Y_{CO} and Y_{CO_2} are the yields to CO and CO_2, respectively, that are defined as:

$$Y_{CO}(\%) = \frac{[CO]_{out}}{2x[TCE]_{in}} \times 100 \quad (11)$$

$$Y_{CO_2}(\%) = \frac{[CO_2]_{out}}{2x[TCE]_{in}} \times 100 \quad (12)$$

Thus, the synergy factor gives the relation of the studied parameter for plasma-catalysis with respect to the sum of its individual values for plasma and catalyst alone conditions. If this value exceeds 1, a synergetic effect is observed.

Table 1 shows that the synergy factor for TCE abatement is in the range of 0.78–1.35, which indicates that the plasma-catalytic system does not offer a clear synergy with respect to the TCE abatement. Moreover, this factor decreases with the temperature in the oven. This is reasonable because at higher temperatures, the catalyst efficiency for VOC removal increases. In contrast, the synergy factor for the yields to CO and CO_2 ranges from 1.22 to 4.78, indicating that the plasma-catalytic system greatly enhances the selectivity of the process towards total oxidation.

Table 1
Synergy factors for plasma-catalytic TCE abatement.

Temp (°C)	f_{TCE} 40 J/L	f_{TCE} 80 J/L	f_{CO} 40 J/L	f_{CO} 80 J/L	f_{CO_2} 40 J/L	f_{CO_2} 80 J/L
300	1.35	1.16	4.43	4.78	3.32	3.90
350	0.99	0.97	3.51	3.79	2.64	3.09
400	0.92	0.91	2.48	2.83	1.70	1.97
450	0.89	0.87	1.85	2.23	1.44	1.63
500	0.83	0.78	1.36	1.54	1.22	1.36

3.6. The role of the ozone in TCE abatement by plasma-catalysis

The ozone produced in the discharge plays a very important role for the removal of TCE by the combined use of NTP and catalysis. Diverse oxidation reactions using ozone in the feed gas mixture are well known, e.g. catalytic oxidation of benzene [32,33], toluene [34]

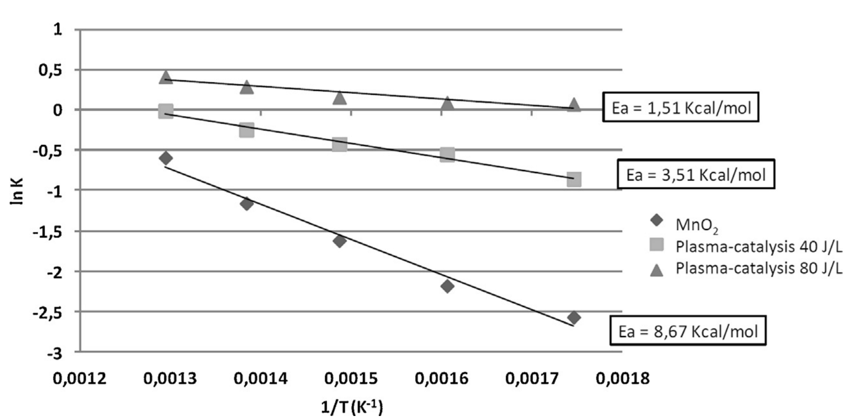

Fig. 6. Arrhenius plot of the influence of temperature on the activity of MnO_2 for plasma-catalytic TCE abatement.

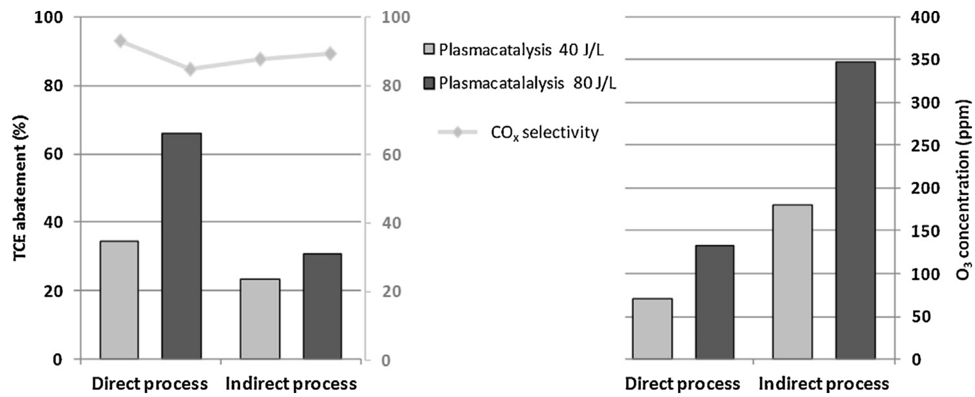

Fig. 7. Influence of the position of TCE inlet on TCE abatement and ozone concentration for plasma-catalysis.

and formaldehyde [35]. In all cases, ozone is cleaved at the surface of the catalyst where it can form peroxide species over the surface [36]:

$$O_3 + (\text{surface}) \rightarrow O_2 + \text{O-(surface)}$$

$$O_3 + \text{O-(surface)} \rightarrow O_2 + O_2\text{-(surface)(Rideal–Eleytypereaction)}$$

To clarify the role of ozone in the plasma-catalytic TCE abatement, the following experiment was carried out. Dry air was fed to the plasma reactor to obtain an ozone concentration of 350 ppm. Next, TCE was introduced in a mixing chamber after the plasma reactor to obtain an ozone/air mixture containing 500 ppm TCE, which was fed to the heated catalyst (indirect process). The ozone concentration was measured at the outlet of the combined system. The TCE abatement and the ozone concentration were compared to the case where the TCE/air mixture was directly fed to the plasma reactor (direct process). In both cases, the temperature in the catalyst bed was maintained at 300 °C. The results obtained in both cases are depicted in Fig. 7.

These experiments provided some useful information about the reaction pathways. The direct process gave a higher TCE abatement than the indirect one, even though the ozone concentration was much higher for the latter one. This is necessarily related to the formation of oxidized compounds in the plasma originating from TCE because a higher concentration of ozone in the reaction mixture should increase the TCE abatement over the catalyst. This is corroborated by two facts. On the one hand, the catalyst gave rise to a higher TCE abatement and CO_x-selectivity for the indirect process than for the catalytic process in absence of plasma discharge (Fig. 7). On the other hand, the TCE abatement of the indirect process was higher for an energy density of 80 J/L than for one of 40 J/L. Consequently, the production of oxygenated intermediates, such as phosgene and DCAC, which are more reactive than TCE, improves the performance of the catalyst. These transformations that occur when TCE is introduced in the plasma entail a significant reduction in the concentration of ozone after the catalyst.

As shown in Fig. 7, the TCE abatement was higher for the direct process. This can be attributed to the fact that for this case energy is transferred to both air and TCE molecules while in the indirect process energy is only transferred to air molecules of the feeding gas. This statement also leads to another conclusion: for the direct process TCE is partially converted to phosgene and DCAC which reach the catalyst surface with a degree of excitation and are therefore more easily decomposed. For the indirect process, however, energy is only transferred to air molecules producing ozone

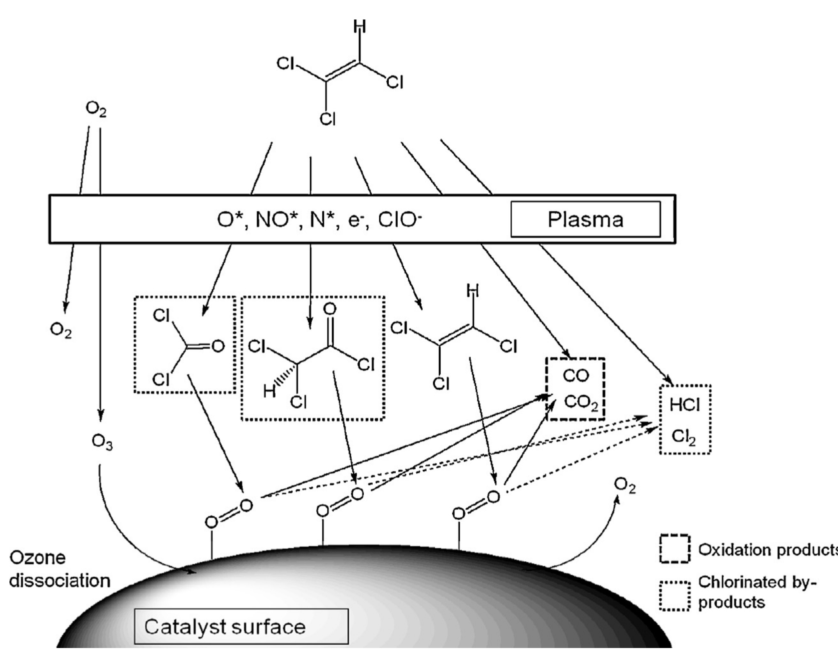

Fig. 8. Plausible reaction pathway for the plasma-catalytic TCE abatement.

which mainly comes together with TCE at the catalyst surface. To support the latter conclusion, the ozone concentration for the indirect process is twice as high compared to the direct process (Fig. 7, right).

3.7. Transformations in TCE abatement by plasma-catalysis

The TCE abatement and selectivity results obtained in the plasma-catalytic configuration and their comparison to those found in either the catalytic or plasma systems suggest a reaction scheme for the TCE abatement that is represented in Fig. 8. Firstly, electron-molecule collisions convert N_2 and O_2 molecules to a mixture of ionized, excited, radical and metastable species that are able to decompose TCE to oxygenated intermediates and final oxidation products. Secondly, ozone dissociates on the catalyst surface to form peroxide groups and molecular oxygen in the gas phase. These surface species promote the complete oxidation of TCE to CO, CO_2, HCl and Cl_2. This oxidation is more efficient if oxygenated molecules, like phosgene and DCAC, arrive to the surface of the catalyst.

4. Conclusions

In this study, we experimentally investigated the abatement of TCE with a plasma-catalytic combined system, formed by a multi-pin-to-plate negative DC corona/glow discharge and MnO_2 catalyst placed downstream of the plasma reactor in a tubular oven.

For the plasma alone system, the main reaction products were oxygenated intermediates (phosgene, DCAC), CO, CO_2, HCl and Cl_2. The CO_x-selectivity did however not exceed 15% even at 240 J/L, indicating that the NTP process is not sufficiently selective.

Under pure catalytic conditions, TCE abatement reached 42.6% at the maximum temperature of 500 °C. The CO_x-selectivity significantly improved when compared to the plasma alone system, thereby minimizing the formation of chlorinated by-products.

The combined application of plasma and catalysis led to an enhancement of TCE abatement compared to the separate systems. Although no clear synergetic effect was found for TCE abatement, the synergy factor for the yield to CO ranged from 1.36 to 4.78 and for CO_2 from 1.22 to 3.90, indicating that the plasma-catalytic system greatly enhances the selectivity of the process towards total oxidation compared to the plasma alone case.

An Arrhenius plot was made in order to calculate the activation energy of the catalytic oxidation and two cases of plasma-catalysis (40–80 J/L). By combining both systems, the activation energy (3.5–1.5 kcal/mol) was significantly decreased compared to pure catalytic conditions (8.7 kcal/mol). This suggests that the oxygenated intermediates (phosgene, DCAC) produced by the plasma are more susceptible for catalytic oxidation than TCE.

For the plasma-catalytic process, the role of ozone was studied by introducing TCE after the discharge. These results showed that the role of ozone, generated in the plasma, is not to increase the TCE abatement, but to offer more oxidizing conditions. The ozone is able to dissociate on the catalyst surface by a Rideal–Eley mechanism, thereby creating peroxide surface groups which greatly improve the oxidation of TCE.

As shown in this study, the combined use of plasma and catalysis is a very interesting route for the abatement of VOCs, using low energy density in the plasma and moderate catalytic temperatures. Therefore, work is currently in progress to study the use of other oxides in order to further increase the efficiency for the total oxidation of chlorinated hydrocarbons.

Acknowledgments

R. Morent acknowledges the support of the Research Foundation Flanders (FWO, Belgium) through a post-doctoral research fellowship.

The research leading to these results has received funding from the European Research Council under the European Union's Seventh Framework Programme (FP/2007-2013)/ERC Grant Agreement n. 279022.

M. Mora acknowledges funding from Junta de Andalucia (FQM-6181), Ministry of Science and Innovation (MAT 2010-18778) and Fondos Feder.

References

[1] C.M. Nunez, G.H. Ramsey, W.H. Ponder, J.H. Abbott, L.E. Hamel, P.H. Kariher, Air Waste 43 (1993) 242–247.
[2] T. Yamamoto, K. Ramaanathan, P.A. Lawless, D.S. Ensor, J.R. Newsome, N. Plaks, R.G.H. Ieee, Trans. Ind. Appl. 28 (1992) 528–534.
[3] A. Ogata, N. Shintani, K. Mizuno, S. Kushiyama, T. Yamamoto, IEEE Trans. Ind. Appl. 35 (1999) 753–759.
[4] U. Roland, F. Holzer, F.D. Kopinke, Catal. Today 73 (2002) 315–323.
[5] J. Van Durme, J. Dewulf, W. Sysmans, C. Leys, H. Van Langenhove, Chemosphere 68 (2007) 1821–1829.
[6] M. Magureanu, N.B. Mandache, V.I. Parvulescu, Plasma Chem. Plasma Process. 27 (2007) 679–690.
[7] R. Morent, C. Leys, J. Dewulf, D. Neirynck, J. Van Durme, H. Van Langenhove, J. Adv. Oxid. Technol. 10 (2007) 127–136.
[8] A.M. Vandenbroucke, R. Morent, N. De Geyter, C. Leys, J. Hazard. Mater. 195 (2011) 30–54.
[9] B. Dhandapani, S.T. Oyama, Appl. Catal. B-Environ. 11 (1997) 129–166.
[10] H. Einaga, S. Futamura, J. Catal. 227 (2004) 304–312.
[11] M.A. Peluso, L.A. Gambaro, E. Pronsato, D. Gazzoli, H.J. Thomas, J.E. Sambeth, Catal. Today 133 (2008) 487–492.
[12] P. Ruetschi, J. Electrochem. Soc. 131 (1984) 2737–2744.
[13] C. Lahousse, A. Bernier, P. Grange, B. Delmon, P. Papaefthimiou, T. Ioannides, X. Verykios, J. Catal. 178 (1998) 214–225.
[14] S. Futamura, A. Gurusamy, J. Electrostat. 63 (2005) 949–954.
[15] J. Jarrige, P. Vervisch, Appl. Catal. B-Environ. 90 (2009) 74–82.
[16] S.B. Han, T. Oda, R. Ono, IEEE Trans. Ind. Appl. 41 (2005) 1343–1349.
[17] Y.S. Akishev, A.A. Deryugin, I.V. Kochetov, A.P. Napartovich, N.I. Trushkin, J. Phys. D-Appl. Phys. 26 (1993) 1630–1637.
[18] Y. Akishev, O. Goossens, T. Callebaut, C. Leys, A. Napartovich, N. Trushkin, J. Phys. D-Appl. Phys. 34 (2001) 2875–2882.
[19] A.M. Vandenbroucke, D. Minh Tuan Nguyen, J.-M. Giraudon, R. Morent, N. De Geyter, J.-F. Lamonier, C. Leys, Plasma Chem. Plasma Process. 31 (2011) 707–718.
[20] M.J. Kirkpatrick, W.C. Finney, B.R. Locke, Plasmas Polym. 8 (2003) 165–177.
[21] S. Futamura, T. Yamamoto, IEEE Trans. Ind. Appl. 33 (1997) 447–453.
[22] M.C. Alvarez-Galvan, B. Pawelec, V.A.D. O'Shea, J.L.G. Fierro, P.L. Arias, Appl. Catal. B-Environ. 51 (2004) 83–91.
[23] E. Finocchio, G. Sapienza, M. Baldi, G. Busca, Appl. Catal. B-Environ. 51 (2004) 143–148.
[24] V.P. Santos, M.F.R. Pereira, J.J.M. Orfao, J.L. Figueiredo, Appl. Catal. B-Environ. 99 (2010) 353–363.
[25] C.M. Su, R.W. Puls, Environ. Sci. Technol. 33 (1999) 163–168.
[26] U. Roland, F. Holzer, E.D. Kopinke, Appl. Catal. B-Environ. 58 (2005) 217–226.
[27] Y.F. Guo, D.Q. Ye, K.F. Chen, J.C. He, W.L. Chen, J. Mol. Catal. A-Chem. 245 (2006) 93–100.
[28] A.M. Harling, V. Demidyuk, S.J. Fischer, J.C. Whitehead, Appl. Catal. B-Environ. 82 (2008) 180–189.
[29] C. Ayrault, J. Barrault, N. Blin-Simiand, F. Jorand, S. Pasquiers, A. Rousseau, J.M. Tatibouet, Catal. Today 89 (2004) 75–81.
[30] A. Baylet, P. Marecot, D. Duprez, X. Jeandel, K. Lombaert, J.M. Tatibouet, Appl. Catal. B-Environ. 113 (2012) 31–36.
[31] A. Maciuca, C. Batiot-Dupeyrat, J.-M. Tatibouet, Appl. Catal. B-Environ. 125 (2012) 432–438.
[32] A. Naydenov, D. Mehandjiev, Appl. Catal. a-Gen. 97 (1993) 17–22.
[33] H. Einaga, A. Ogata, J. Hazard. Mater. 164 (2009) 1236–1241.
[34] E. Rezaei, J. Soltan, Chem. Eng. J. 198 (2012) 482–490.
[35] D.-Z. Zhao, C. Shi, X.-S. Li, A.-M. Zhu, B.W.L. Jang, J. Hazard. Mater. 239 (2012) 362–369.
[36] W. Li, G.V. Gibbs, S.T. Oyama, J. Am. Chem. Soc. 120 (1998) 9041–9046.